

Penetration depth of electron-doped infinite-layer $\text{Sr}_{0.88}\text{La}_{0.12}\text{CuO}_{2+x}$ thin filmsL. Fruchter,¹ V. Jovanovic,² H. Raffy,¹ Sid Labdi,³ F. Bouquet,¹ and Z. Z. Li¹¹*Laboratoire de Physique des Solides, Univ. Paris-Sud-CNRS, UMR 8502, F-91405 Orsay Cedex, France*²*Institute of Physics, Pregrevaica 118, Belgrade, Serbia*³*Laboratoire des Milieux Nanométriques, Université d'Evry, 91025 Evry Cedex, France*

(Received 18 February 2010; revised manuscript received 24 September 2010; published 28 October 2010)

The in-plane penetration depth of $\text{Sr}_{0.88}\text{La}_{0.12}\text{CuO}_{2+x}$ thin films at various doping obtained from oxygen reduction has been measured, using ac-susceptibility measurements. For the higher doping samples, the superfluid density deviates strongly from the *s*-wave behavior, suggesting, in analogy with other electron-doped cuprates, a contribution from a nodal hole pocket, or a small gap on the Fermi surface such as an anisotropic *s*-wave order parameter. The low value of the superfluid densities, likely due to a strong doping-induced disorder, places the superconducting transition of our samples in the phase-fluctuation regime.

DOI: [10.1103/PhysRevB.82.144529](https://doi.org/10.1103/PhysRevB.82.144529)

PACS number(s): 74.72.Ek, 74.25.N–

The question whether superconductivity obtained by doping the CuO_2 planes in hole-doped and electron-doped cuprates involves the same mechanisms is still a matter of debate. Indeed, evidences for asymmetry of the electronic properties between electron- and hole-doped compounds have been pointed out long ago, some of them still controversial.

First, the antiferromagnetic (AFM) order common to both systems at very low doping has often been reported to extend to a much higher doping range for electron-doped materials and found to overlap with the superconducting dome.¹ However, this description is challenged by recent neutron-diffraction studies that conclude that genuine long-range antiferromagnetism and superconductivity do not coexist.² On a theoretical point of view, a phase separation into a mixed antiferromagnetic and superconducting (SC) phase has been predicted for both classes of materials (although with a much larger energy scale in the case of hole doped)³ while several experimental findings could be interpreted within a model that assumes coexisting AFM and SC orders.^{4,5}

Then, one of the essential characteristics of the hole-doped cuprate superconductivity is the *d*-wave symmetry of its order parameter, believed to reflect the pairing mechanism. In the electron-doped case (e-doped case), *d*-wave symmetry has been evidenced by several high-quality experimental contributions, however, several others point toward a dominant *s*-wave order parameter (for a review, see Ref. 6). Recently, it has been proposed that this complexity may originate from the fact that, although e-doped cuprates properties for samples below optimal doping are indeed dominated by the electron pockets of the Fermi surface, hole pockets are developing as the doping is increased and may actually become dominant. The interplay between the doping evolution of the Fermi surface and a *d*-wave order parameter would then yield the rich behavior as a function of doping of the e-doped family.^{4,5} Some authors go further and suggest that, in the case of e-doped $\text{Pr}_{2-x}\text{Ce}_x\text{CuO}_4$ (PCCO), electrons may have no role in the occurrence of superconductivity, which would then be entirely dominated by the contribution of the hole pockets.⁷

Confronted to this debated situation, experimental clues brought by an additional member of the restricted e-doped family—the so-called “infinite phase” $\text{Sr}_{1-x}\text{La}_x\text{CuO}_2$

(SLCO)—may prove useful. Concerning the issue of the order-parameter symmetry, there have been several experimental investigations for this material, most of them pointing toward a dominant *s*-wave superconducting order in the case of optimally doped SLCO: the lack of a momentum dependence, as well as of a zero-bias conductance peak, in tunneling spectroscopy;⁸ the temperature and magnetic field scaling of the mixed state specific heat;⁹ the local-field distribution from low-angle neutron diffraction by the flux-line lattice;¹⁰ the muon-spin-rotation measurements of the flux-line-lattice field distribution.⁶ However, other measurements found a temperature or a magnetic field dependence indicative of nodes in the gap.^{11,12} It was also pointed out that, in a similar way to what is observed for other e-doped cuprates, the zero-temperature superfluid density in SLCO does not follow the “universal” Uemura line for optimally hole-doped cuprates,^{11–13} due to much shorter penetration depth for comparable superconducting-transition temperatures. This tends to indicate that, for the e-doped cuprates, the Fermi-liquid regime extends over a larger doping range than for the hole-doped cuprates,¹² in apparent contradiction with antiferromagnetism extending further into the underdoped regime.

In the present study, we report measurements of the magnetic penetration depth of SLCO thin films. Despite its structural simplicity— CuO_2 layers alternating with $\text{Sr}_{1-x}\text{La}_x$ layers—SLCO is difficult to fabricate. As a bulk material, it can only be synthesized under pressure, and no single crystal could be grown up to now. As a thin film, epitaxial growth of *c*-axis-oriented SLCO was, however, made possible by the use of the appropriate substrate.^{14–16} We have grown by rf magnetron sputtering several $\text{Sr}_{1-x}\text{La}_x\text{CuO}_2$ ($x=0.12$) thin films, approximately 400 Å thick on $5 \times 5 \text{ mm}^2$ (100) KTaO_3 substrates. The CuO_2 planes doping with electrons is provided here both by the $\text{Sr}^{2+}/\text{La}^{3+}$ substitution (which was kept constant in this study) but also by an oxygen content reduction; indeed, during the process additional oxygen atoms enter the structure, most probably within the $\text{Sr}^{2+}/\text{La}^{3+}$ planes. The samples were annealed *in situ* during the cooling procedure after deposition; the final doping state of a sample is determined by the temperature of annealing or its conditions (under vacuum or argon pressure), the lower oxygen content resulting in a higher doping. In a last step, a cover—approximately 100 Å thick—of amorphous, insulating, ma-

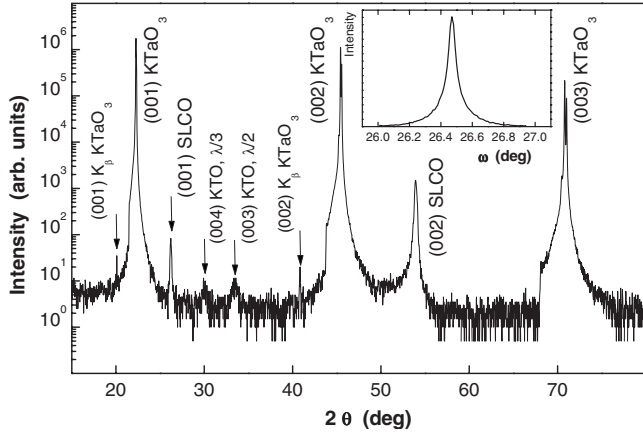


FIG. 1. Cu $K\alpha$ x-ray θ - 2θ diffraction scan, for a 590-Å-thick film. The inset is the rocking curve for the (002) peak, showing a mid-height width of 0.07 degree.

material was deposited, to ensure optimum stability of the film. We obtained thin films with T_c up to 19 K for the lower oxygen content. Using Cu $K\alpha$ x-ray diffraction, the thickness of each film was measured from the low-angle Kiessig fringes, and the absence of parasitic phases was checked from conventional θ - 2θ pattern (see Fig. 1).

The penetration depth λ was measured using an ac susceptometer setup based on Ref. 17. It was built using two identical astatically wound pairs, each made from 1.25 mm diameter, 100 turn coils. The use of quadrupoles minimizes the sample finite-size contribution to the background signal, which was measured using a thick Nb sample with the same dimensions as the measured films. The mutual inductance ($M_1 + iM_2$) corrected from the finite-size effects was obtained using the procedure described in Ref. 18 (Fig. 2). The geometry of the coils, combined with the relatively small thickness of the measured films (thinner than λ), allowed for an accurate determination of the mutual inductance on the whole temperature range. This is necessary for a reliable determination of the penetration-depth temperature dependence: at the lowest temperature that could be reached by our apparatus (4 K), the out-of-phase signal was always larger than about 6% of the signal above T_c , and twice as large as the correction brought by the background signal. The latter was independent of the temperature in our range: the tem-

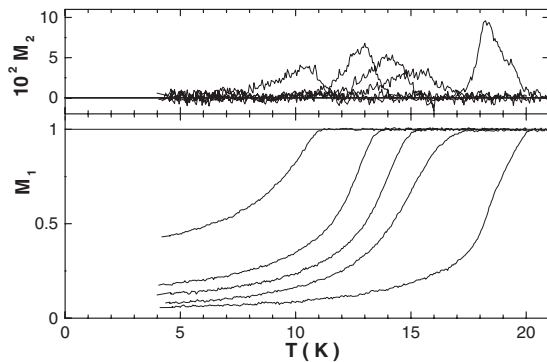


FIG. 2. Normalized in-phase (M_2) and out-of-phase (M_1) pickup signal for films with $T_c = 19, 15, 14, 13,$ and 11 K.

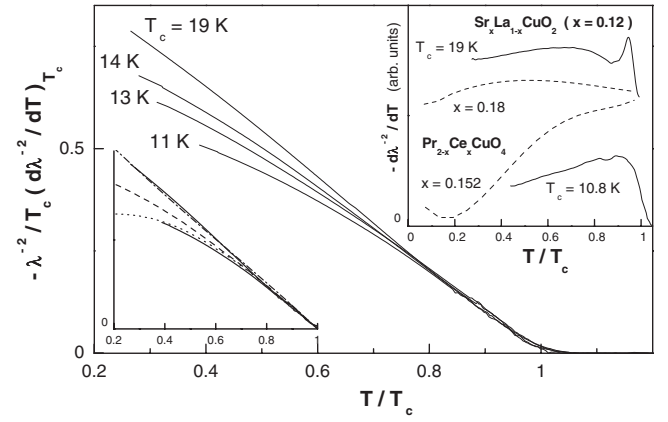


FIG. 3. Squared inverse of the penetration depth, as obtained from the mutual inductance in Fig. 2, normalized to the slope at T_c . The bottom inset is an attempt to fit the $T_c = 19$ K data (upper full line) and the $T_c = 11$ K data (lower full line) to clean s -wave (dotted line), d -wave (dashed line) and anisotropic s -wave (dashed dotted) theory. The top inset shows the temperature derivative for these two same samples (full lines); for comparison data from Ref. 5 are also plotted, corresponding to an optimally doped ($x = 0.152$) and overdoped ($x = 0.18$) $\text{Pr}_{2-x}\text{Ce}_x\text{CuO}_4$.

perature of the measurement setup was kept constant and independent of the sample temperature during measurement. The value of the ac field at 50 kHz was adjusted in order to remain in the linear regime, where the measured inductance is independent of the excitation of the driving coil. Using a lookup table computed for the specific geometry of our setup, the penetration depth was obtained from the complex mutual inductance. T_c was obtained from a linear extrapolation of $\lambda^{-2}(T)$ to zero.

As can be seen in Fig. 3, the curvature for $\lambda^{-2}(T)$ is found to decrease as doping increases. Although our limiting temperature is too large to determine the asymptotic behavior for $\lambda^{-2}(T \rightarrow 0)$, it may be asserted that, for the higher dopings in Fig. 3, the curvature at low temperature is too weak to allow for a fit with a clean isotropic s -wave model, unlike for the lower doping (Fig. 3, bottom inset). In the case of the strongest doping, quasilinear behavior does not either allow for a fit using a d -wave model. Such a quasilinear behavior may be obtained down to $T_c \approx 0.3$, as observed here, provided there is a sufficiently small gap on the Fermi surface. This is the case of the anisotropic s -wave model. Restricting ourselves to the weak-coupling limit and standard fourfold asymmetry, the gap can be expressed as $\Delta(T, \varphi) = \Delta_0 \Delta(T/T_c) [1 + a \cos(4\varphi)] / (1 + a)$, where φ is the angle within the planes, $a \leq 1$ measures the anisotropy, $\Delta_0 = 1.76k_B T_c (1 + a)(1 - 3a/4)$ is the maximum gap on the Fermi surface,¹⁹ and $\Delta(T/T_c)$ is the reduced BCS temperature dependence.²⁰ A reasonable fit is obtained for our sample with higher doping, using $a = 0.65 \pm 0.05$; this large a implies that the smallest value of the gap at the Fermi surface is only 20% of Δ_0 . Introducing strong-coupling effects would increase the value of a .

Reference 5 proposes a competing two-band model: the behavior close to linear for $T/T_c > 0.25$ which has been reported for overdoped PCCO is attributed to the merging of

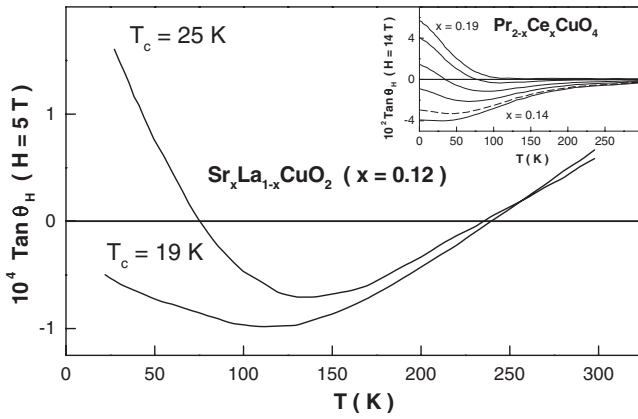


FIG. 4. Hall angle for underdoped SLCO, as obtained from the data in Refs. 16 and 22. Inset: for PCCO, as computed from a mixing of underdoped and overdoped experimental data (Refs. 5 and 7) ($x=0.14, 0.15, 0.155, 0.16, 0.18, 0.19$); the dashed line is for optimal doping.

an electron and a hole pocket of the Fermi surface into a single nodal hole pocket as the doping increases. Due to a similar evolution of the Fermi surface with doping, an analogous behavior might also be expected in the case of $\text{Nd}_{2-x}\text{Ce}_x\text{CuO}_4$ (NCCO).^{5,21} In the present case, a close examination of $\lambda^{-2}(T)$ (Fig. 3, top inset) reveals further similarity with PCCO: for the higher doping also, $\lambda^{-2}(T)$ exhibits an *upward* curvature for the higher temperatures, and a *downward* one for the lower ones (disregarding the regime close to T_c , which may be influenced by intrinsic or extrinsic factors). *A contrario*, both optimally doped PCCO and the lower SLCO doping state appear to show a *downward* curvature in the whole temperature range. Within the two-bands model, the change in curvature for $\lambda^{-2}(T)$ arises from the mixing of the contribution to the superfluid density of the nodal hole pocket (showing upward curvature) and of the one of the antinodal electron pocket (showing downward curvature).⁵

Additional evidence for a contribution of a hole pocket is found from the comparison of the electronic transport properties for both materials. As can be seen in Fig. 4, the Hall angle for SLCO contains a positive contribution that becomes larger as the temperature decreases and becomes positive for the highest T_c . A very similar behavior was observed in PCCO (see Fig. 4), even though the value of the Hall effect is smaller by two orders of magnitude, indicating a much lower scattering. This behavior of the Hall angle at low temperature was interpreted as the signature of the hole pocket existence at the Fermi surface. Despite the difference of value, the similarity of the temperature dependence of the Hall effect in our samples is consistent with the existence of such a hole pocket in SLCO, with a contribution that grows larger as the doping is increased. Thus, while the monotonic increase of T_c with doping suggests that all our samples are still in the underdoped state, data in Fig. 4 show a similar behavior to what is observed in *overdoped* PCCO.

One may first question these observations as being intrinsic properties of SLCO. Our films may differ from the bulk material in several ways. First, SLCO films epitaxially

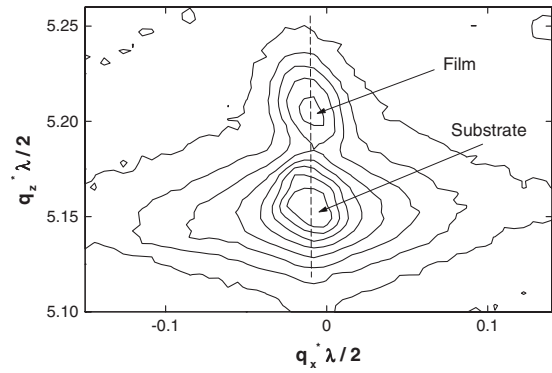


FIG. 5. Contour plot (log scale) for a ω - 2θ scan in the vicinity of the (411) reflection, showing alignment of the film and substrate peaks, indicative of a fully constrained film, for a 400-Å-thick film. Dashed line is a guide to the eyes.

grown on (100) KTaO_3 substrates are likely highly stressed. The substrate parameter for KTaO_3 is 3.989 Å while the basal-plane parameter reported for bulk SLCO is $a=b=3.95$ Å.²³ Large parameter mismatch may have no consequence for soft materials; for instance, Bi-based cuprates [basal parameter 3.79–3.83 Å, Young's modulus $E \approx 40$ GPa (Ref. 24)] may be epitaxially grown on a variety of substrates, ranging from SrTiO_3 , $a=3.905$ Å, to MgO , $a=4.21$ Å. However, the compact crystallographic cell of SLCO would rather indicate a large Young's modulus. Indeed, we have noticed that our films, if submitted to a local mechanical stress, may delaminate, leaving a patchwork of free standing and epitaxial film zones, that, in turn, induce local twinning of the substrate. Such an observation is usually a manifestation of highly stressed films.

The Young's modulus of one of our films has been determined from nanoindentation measurements, using Oliver and Pharr elastoplastic model,²⁵ yielding $E=280 \pm 10$ GPa. The small thickness of the films probably does not allow the stress to relax. Indeed, assuming a uniformly stressed, isotropic film and taking for the strain in the basal plane the difference between the substrate parameter and the bulk-SLCO parameter, ($\epsilon_{\parallel}=9.9 \times 10^{-3}$), and for the transverse one the difference between the bulk value $c=3.42$ Å and the one measured for our films, $c=3.398$ Å, ($\epsilon_{\perp}=-6.4 \times 10^{-3}$), we obtain the Poisson ratio $\nu = -(\epsilon_{\perp} / \epsilon_{\parallel}) / (2 - \epsilon_{\perp} / \epsilon_{\parallel}) = 0.24$, which is quite a reasonable value, as compared to simple oxides or cuprates.²⁶

In addition, we performed ω - 2θ x-ray diffraction scans. They showed an alignment of the substrate and the film peaks, which is characteristic of an unrelaxed epitaxial thin film (Fig. 5). This is in line with several observations showing that oxides films need a much larger thickness to relax than would be predicted from thermodynamic models.²⁷ Using the modulus measured for our films, a uniform stress about 3 GPa is expected, which may modify the band structure from relaxed bulk SLCO. The simplest effect for such a band-structure modification would likely be to shift the doping state (toward higher doping, as we have seen above); however, we failed to observe a decrease of T_c with doping, as would be expected in the overdoped regime.

Then, doping with oxygen may not be equivalent to dop-

ing with Sr/La substitution. Additional oxygen atoms into the $\text{Sr}_{1-x}\text{La}_x$ layers also introduce Cu-O bonds between CuO_2 planes, via the apical oxygen, that are not present in the original material. While it is known that oxygen vacancies present in distant charge-reservoir planes or chains may locally alter the electronic properties of the conducting planes,²⁸ such a proximity of the doping atom may have dramatic effects, eventually resulting in inhomogeneous superconductivity. In the case of $\text{Sr}_2\text{CuO}_{3+x}$, it was shown that ordering of the apical oxygen has a noticeable effect on the superconducting transition temperature, in the absence of a change of the doping in the CuO_2 planes,²⁹ as also has disorder in the adjacent SrO plane for Bi-based compounds.³⁰ Previous studies have shown that our SLCO films with larger oxygen content have larger transition width, as the zero-resistance temperature experiences larger shift with oxygen content than the onset temperature does. Within this perspective, it is reasonable to assume that oxygen content alters both doping and disorder. Disorder can have a strong effect on both the superconducting temperature and the superfluid density, when nodes are present in the order parameter. It has indeed be noticed, in the case of PCCO, that the values computed for $\lambda(0)$ are well below the experimental ones, suggesting also a doping-induced disorder.⁴ For SLCO, the effect should be stronger, due to the specific position of the doping oxygen.

Given that our samples are strongly disordered, the behavior of $\lambda(T)^{-2}$ should be affected. It is indeed well known that, for a d -wave superconductor, scattering induces a finite density of states at the Fermi level and changes the zero-temperature asymptotic behavior from a linear to a quadratic law in temperature whereas, above some crossover temperature, the pure regime is recovered.³¹ By analogy, within the two-bands model, one would expect the contribution of the hole pocket that carries the d -wave character of the superconductivity to be strongly affected by disorder. However, our measurements do not cover the low-temperature range where disorder should dominate the λ^{-2} behavior. Indeed, our analysis is made for $T/T_c \geq 0.3$, where the contribution of disorder is expected to be negligible. There are indications, from the available data on cuprates with a simpler Fermi surface, that one may simultaneously observe a strong reduction of both T_c and the superfluid density due to disorder, and a temperature behavior for $\lambda(T)$ reminiscent of their d -wave character, in such a high-temperature regime (see, e.g., Ref. 32, where a YBa_2CuO_7 thin film substituted by 6% Ni exhibits superfluid density reduced by a factor 25 and T_c reduced by a factor 1.3 while above $T/T_c \approx 0.3$, the pure d -wave result provides a good fit to the data; see also Ref. 33). Although the Fermi surface of our electron-doped compound is more complex than that of hole-doped cuprates, we similarly expect that the high-temperature pure behavior is preserved in the present case. Thus, although the details of the Fermi surface also contribute to the high-temperature behavior of the superfluid density and may introduce some discrepancy with respect to the conventional d -wave result for a single cylindrical Fermi surface, we consider the strong departure from the s -wave result (Fig. 3) as a possible contribution from a nodal band.

Finally, we comment on the $T_c - \lambda^{-2}(0)$ relationship. Even

TABLE I. $[d\lambda^{-2}(T)/dT]_{T_c}$ and extrapolated values for $\lambda(T=0)$, as explained in the text.

T_c (K)	$-10^2[d\lambda^{-2}(T)/dT]_{T_c}$ ($\mu\text{m}^{-2} \text{K}^{-1}$)	$\lambda(T=0)$ (μm)
7.1	0.43	7.1
10.8	2.4	2.2
12	2.6	2.1
13	6.8	1.2
14.3	8.1	1.0
14.9	11.3	0.85
19	11.4	0.69

though the lowest available temperature is 4 K, the temperature range of our experiment is enough to allow the estimation of $\lambda^{-2}(0)$ by extrapolating $\lambda^{-2}(T)$. This may be done either using a linear extrapolation or a quadratic one, which yields close results (the averaged values are presented in Table I and Fig. 6). These extrapolated values for $\lambda(0)$ (Fig. 6) are much larger than what has been previously measured in bulk SLCO near optimal doping.^{6,12} T_c is found to extrapolate to zero as $(\lambda^{-2}(0))^\alpha$, where $\alpha \approx 0.2$ (Fig. 6, inset). The data strongly suggest a crossover to a phase-fluctuation regime, as $1/\lambda(0)^2 \rightarrow 0$, when the superfluid density is low enough to impose a superconducting transition driven by phase ordering. The fluctuations may be of thermal origin or driven by the proximity of a quantum critical point (QCP).³⁹ In the case of a QCP, a sublinear dependence is expected, as observed in our case (Fig. 6, inset). However, both quantities are expected to be related as $T_c \propto [1/\lambda(0)^2]^\alpha$, where $\alpha = z/(z+D-2)$, $z \geq 1$ (see, e.g., Ref. 40 and references therein) and $D=3$ in the present case, owing to comparable interplane distance and coherence length.¹⁶ The resulting value, $z \approx 0.25$, is an unphysically small, making the QCP scenario unlikely. The phase-fluctuation scenario should be favored

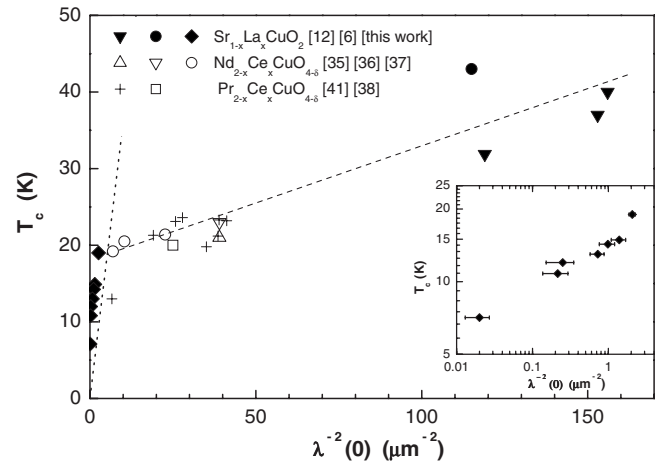


FIG. 6. T_c vs $\lambda^{-2}(T=0)$ for various e-doped cuprates. The dotted line is the Uemura line for moderately underdoped hole-doped cuprates (Ref. 34); the dashed line is a guide to the eyes. Inset: log-log representation of our data, where the error bars are estimated from the different methods of $\lambda(0)$ extrapolation. These data follow $T_c \propto [\lambda^2(0)]^{-0.2}$ (Refs. 35–38).

by weak phase stiffness and a short coherence length. SLCO [as well as NCCO (Ref. 41)] shows a smaller upper critical field than hole-doped cuprates [$dB_{c2}/dT \approx 0.3 \text{ T K}^{-1}$ (Ref. 6) and 0.5 T K^{-1} (Ref. 16) while $dB_{c2}/dT \approx 2 \text{ T K}^{-1}$ for hole-doped cuprates] and a relatively small penetration depth (Fig. 6): this does not make it a likely candidate for the phase-fluctuation scenario, as found in Ref. 12. However, with decreasing doping in the e-doped materials, the antinodal carriers become dominant, for which there is a finite coherence length (as opposed to the nodal direction) while there is an decrease of the superfluid density (due to the reduction in the carrier density and/or stronger disorder): both effects could then favor a crossover from a conventional mean-field behavior to a superconducting transition driven by phase fluctuations. The linear $T_c - \lambda^{-2}(0)$ relationship, which is thought to be characteristic of this mechanism,³⁴ is, however, also not observed by us. Finally, an alternative universal scaling was proposed in Ref. 42, linearly relating the superfluid density to the product $\sigma_{DC}T_c$. Alternatively, it may be viewed as relating the scattering rate at T_c to this parameter. We observe that our data—with the exception of the sample with the lower T_c —obey such a scaling reasonably well (Fig. 7), being situated at the opposite of the large $\sigma_{DC}T_c$ product of metal superconductors.

In summary, the penetration depth of thin films infinite-layer $\text{Sr}_{0.88}\text{La}_{0.12}\text{CuO}_{2+x}$ thin films is found to depart from the isotropic s -wave behavior as doping is increased, indicating the contribution of a smaller gap on the Fermi surface. Both an anisotropic s -wave order parameter and a two-band model, as was used for overdoped $\text{Pr}_{2-x}\text{Ce}_x\text{CuO}_4$, may account for the data. In the latter case, the small gap originates from a nodal hole pocket with a d -wave character.⁵ Large

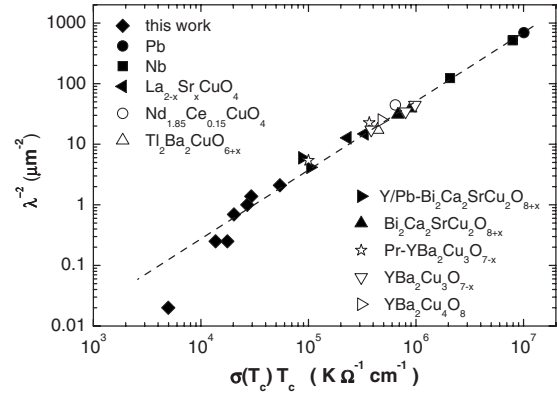


FIG. 7. Full circles: universal scaling for various cuprates and metals, as proposed in Ref. 42 (in-plane conductivities, from the supplementary information). Diamonds: this work (the conductivity is estimated from the data in Ref. 16). Dashed line is a guide to eyes.

values of the zero-temperature penetration depth are observed. Disorder on the apical oxygen site and the associated strong scattering in the CuO_2 plane may be the primary cause for the superfluid density reduction.

ACKNOWLEDGMENTS

The authors are grateful to T. R. Lemberger for sharing valuable knowledge on the ac susceptibility technique. The Orsay group acknowledge the support of the ANR under Project No. ANR-07-BLAN-0242-CSD 4.

- ¹P. Dai, H. J. Kang, H. A. Mook, M. Matsuura, J. W. Lynn, Y. Kurita, S. Komiya, and Y. Ando, *Phys. Rev. B* **71**, 100502(R) (2005).
- ²E. M. Motoyama, G. Yu, I. M. Vishik, O. P. Vajk, P. K. Mang, and M. Greven, *Nature (London)* **445**, 186 (2007).
- ³M. Aichhorn, E. Arrighoni, M. Potthoff, and W. Hanke, *Phys. Rev. B* **74**, 024508 (2006).
- ⁴T. Das, R. S. Markiewicz, and A. Bansil, *Phys. Rev. Lett.* **98**, 197004 (2007).
- ⁵T. Das, R. S. Markiewicz, and A. Bansil, *J. Phys. Chem. Solids* **69**, 2963 (2008).
- ⁶R. Khasanov, A. Shengelaya, A. Maisuradze, D. Di Castro, I. M. Savic, S. Weyeneth, M. S. Park, D. J. Jang, S.-I. Lee, and H. Keller, *Phys. Rev. B* **77**, 184512 (2008).
- ⁷Y. Dagan and R. L. Greene, *Phys. Rev. B* **76**, 024506 (2007).
- ⁸C.-T. Chen, P. Senor, N.-C. Yeh, R. P. Vasquez, L. D. Bell, C. U. Jung, J. Y. Kim, M.-S. Park, H.-J. Kim, and S.-I. Lee, *Phys. Rev. Lett.* **88**, 227002 (2002).
- ⁹Z. Y. Liu, H. H. Wen, L. Shan, H. P. Yang, X. F. Lu, H. Gao, M.-S. Park, C. U. Jung, and S.-I. Lee, *Europhys. Lett.* **69**, 263 (2005).
- ¹⁰J. S. White, E. M. Forgan, M. Laver, P. S. Häfliger, R. Khasanov, R. Cubitt, C. D. Dewhurst, M.-S. Park, D.-J. Jang, H.-G. Lee, and S.-I. Lee, *J. Phys.: Condens. Matter* **20**, 104237 (2008).

- ¹¹A. Shengelaya, R. Khasanov, D. G. Eshchenko, D. Di Castro, I. M. Savic, M. S. Park, K. H. Kim, S.-I. Lee, K. A. Muller, and H. Keller, *Phys. Rev. Lett.* **94**, 127001 (2005).
- ¹²K. H. Satoh, S. Takeshita, A. Koda, R. Kadono, K. Ishida, S. Pyon, T. Sasagawa, and H. Takagi, *Phys. Rev. B* **77**, 224503 (2008).
- ¹³Y. J. Uemura, L. P. Le, G. M. Luke, B. J. Sternlieb, W. D. Wu, J. H. Brewer, T. M. Riseman, C. L. Seaman, M. B. Maple, M. Ishikawa, D. G. Hinks, J. D. Jorgensen, G. Saito, and H. Yamochi, *Phys. Rev. Lett.* **66**, 2665 (1991).
- ¹⁴S.-i. Karimoto, K. Ueda, M. Naito, and T. Imai, *Appl. Phys. Lett.* **79**, 2767 (2001); S.-i. Karimoto and M. Naito, *ibid.* **84**, 2136 (2004).
- ¹⁵Z. Z. Li, V. Jovanovic, H. Raffy, and S. Megtert, *Physica C* **469**, 73 (2009).
- ¹⁶V. Jovanovic, Z. Z. Li, F. Bouquet, L. Fruchter, and H. Raffy, *J. Phys.: Conf. Ser.* **150**, 052086 (2009).
- ¹⁷A. Fiory, A. Hebard, P. Mankiewich, and R. Howard, *Appl. Phys. Lett.* **52**, 2165 (1988).
- ¹⁸S. J. Turneaure, A. A. Pesetski, and T. R. Lemberger, *J. Appl. Phys.* **83**, 4334 (1998).
- ¹⁹J. R. Clem, *Ann. Phys.* **40**, 268 (1966).
- ²⁰A. Carrington and F. Manzano, *Physica C* **385**, 205 (2003).
- ²¹C. Kusko, R. S. Markiewicz, M. Lindroos, and A. Bansil, *Phys.*

- Rev. B* **66**, 140513(R) (2002).
- ²²V. Jovanovic (private communication), the sample with $T_c = 19$ K is sample 3 in Ref. 16.
- ²³J. D. Jorgensen, P. G. Radaelli, D. G. Hinks, J. L. Wagner, S. Kikkawa, G. Er, and F. Kanamaru, *Phys. Rev. B* **47**, 14654 (1993).
- ²⁴Y. He, J. Xiang, S. Jin, A. He, and J. Zhang, *Physica B* **165-166**, 1283 (1990).
- ²⁵W. C. Oliver and G. M. Pharr, *J. Mater. Res.* **7**, 1564 (1992).
- ²⁶E. J. Tarsa, E. A. Hachfeld, F. T. Quinlan, J. S. Speck, and M. Eddy, *Appl. Phys. Lett.* **68**, 490 (1996); F. Nakamura, T. Goko, J. Hori, Y. Uno, N. Kikugawa, and T. Fujita, *Phys. Rev. B* **61**, 107 (2000); J. H. Cheon, P. S. Shankar and J. P. Singh, *Supercond. Sci. Technol.* **18**, 142 (2005).
- ²⁷N. J. C. Ingle, R. H. Hammond, and M. R. Beasley, *J. Appl. Phys.* **91**, 6371 (2002).
- ²⁸K. McElroy, J. Lee, J. A. Slezak, D.-H. Lee, H. Eisaki, S. Uchida, and J. C. Davis, *Science* **309**, 1048 (2005).
- ²⁹Q. Q. Liu, H. Yang, X. M. Qin, Y. Yu, L. X. Yang, F. Y. Li, R. C. Yu, C. Q. Jin, and S. Uchida, *Phys. Rev. B* **74**, 100506(R) (2006).
- ³⁰K. Fujita, T. Noda, K. M. Kojima, H. Eisaki, and S. Uchida, *Phys. Rev. Lett.* **95**, 097006 (2005).
- ³¹P. J. Hirschfeld and N. Goldenfeld, *Phys. Rev. B* **48**, 4219 (1993); P. J. Hirschfeld, W. O. Putikka, and D. J. Scalapino, *ibid.* **50**, 10250 (1994).
- ³²E. R. Ulm, J.-T. Kim, T. R. Lemberger, S. R. Foltyn, and X. Wu, *Phys. Rev. B* **51**, 9193 (1995).
- ³³M. Salluzzo, A. Andreone, F. Palomba, G. Pica, R. Vaglio, I. Maggio-Aprile, and Ø. Fischer, *Eur. Phys. J. B* **24**, 177 (2001).
- ³⁴Y. J. Uemura, G. M. Luke, B. J. Sternlieb, J. H. Brewer, J. F. Carolan, W. N. Hardy, R. Kadono, J. R. Kempton, R. F. Kiefl, S. R. Kreitzman, P. Mulhern, T. M. Riseman, D. Li Williams, B. X. Yang, S. Uchida, H. Takagi, J. Gopalakrishnan, A. W. Sleight, M. A. Subramanian, C. L. Chien, M. Z. Cieplak, Gang Xiao, V. Y. Lee, B. W. Statt, C. E. Stronach, W. J. Kossler, and X. H. Yu, *Phys. Rev. Lett.* **62**, 2317 (1989).
- ³⁵A. A. Nugroho, I. M. Sutjahja, A. Rusydi, M. O. Tjia, A. A. Menovsky, F. R. de Boer, and J. J. M. Franse, *Phys. Rev. B* **60**, 15384 (1999).
- ³⁶C. C. Homes, B. P. Clayman, J. L. Peng, and R. L. Greene, *Phys. Rev. B* **56**, 5525 (1997).
- ³⁷F. Gollnik and M. Naito, *Phys. Rev. B* **58**, 11734 (1998).
- ³⁸C. C. Homes, R. P. S. M. Lobo, P. Fournier, A. Zimmers, and R. L. Greene, *Phys. Rev. B* **74**, 214515 (2006).
- ³⁹V. J. Emery and S. A. Kivelson, *Phys. Rev. Lett.* **74**, 3253 (1995).
- ⁴⁰I. Hetel, T. R. Lemberger, and M. Randeria, *Nat. Phys.* **3**, 700 (2007); D. M. Broun, W. A. Huttema, P. J. Turner, S. Ozcan, B. Morgan, R. Liang, W. N. Hardy, and D. A. Bonn, *Phys. Rev. Lett.* **99**, 237003 (2007).
- ⁴¹M.-S. Kim, J. A. Skinta, T. R. Lemberger, A. Tsukada, and M. Naito, *Phys. Rev. Lett.* **91**, 087001 (2003).
- ⁴²C. C. Homes, S. V. Dordevic, M. Strongin, D. A. Bonn, R. Liang, W. N. Hardy, S. Komiyama, Y. Ando, G. Yu, N. Kaneko, X. Zhao, M. Greven, D. N. Basov, and T. Timusk, *Nature (London)* **430**, 539 (2004).